Small and large intestine express a truncated Dab1 isoform that assembles in cell-cell junctions and co-localizes with proteins involved in endocytosis

María D. Vázquez-Carretero, Pablo García-Miranda, María S. Balda, Karl Matter, María J. Peral, Anunciación A. Ilundain

PII: S0005-2736(18)30055-5
DOI: doi:10.1016/j.bbamem.2018.02.014
Reference: BBAMEM 82708

To appear in:

Received date: 2 November 2017
Revised date: 2 February 2018
Accepted date: 14 February 2018

Please cite this article as: María D. Vázquez-Carretero, Pablo García-Miranda, María S. Balda, Karl Matter, María J. Peral, Anunciación A. Ilundain , Small and large intestine express a truncated Dab1 isoform that assembles in cell-cell junctions and co-localizes with proteins involved in endocytosis. The address for the corresponding author was captured as affiliation for all authors. Please check if appropriate. Bbamem(2018), doi:10.1016/j.bbamem.2018.02.014

Small and large intestine express a truncated Dab1 isoform that assembles in cell-cell junctions and co-localizes with proteins involved in endocytosis

María D. Vázquez-Carretero[a], Pablo García-Miranda[a], María S. Balda[b], Karl Matter[b], María J. Peral[a,*] and Anunciación A. Ilundain[a]

[a] Departamento de Fisiología, Facultad de Farmacia, Universidad de Sevilla, Spain

[b] Department of Cell Biology, Institute of Ophthalmology, University College London, United Kingdom

*Corresponding author: María J. Peral
Departamento de Fisiología, Facultad de Farmacia, Universidad de Sevilla, Spain
C/ Profesor García González, nº 2
41012 Sevilla, Spain.
Telephone: 34 954556177
Email address: mjperal@us.es

ABSTRACT

Disabled-1 (Dab1) is an essential intracellular adaptor protein in the reelin pathway. Our previous studies in mice intestine showed that Dab1 transmits the reelin signal to cytosolic signalling pathways. Here, we determine the Dab1 isoform expressed in rodent small and large intestine, its subcellular location and co-localization with clathrin, caveolin-1 and N-Wasp. PCR and sequencing analysis reveal that rodent small and large intestine express a Dab1 isoform that misses three (Y^{198}, Y^{200} and Y^{220}) of the five tyrosine phosphorylation sites present in brain Dab1 isoform (canonical) and contains nuclear localization and export signals. Western blot assays show that both, crypts, which shelter progenitor cells, and enterocytes express the same Dab1 isoform, suggesting that epithelial cell differentiation does not regulate intestinal generation of alternatively spliced Dab1 variants. They also reveal that the canonical and the intestinal Dab1 isoforms differ in their total degree of phosphorylation. Immunostaining assays show that in enterocytes Dab1 localizes at the apical and lateral membranes, apical vesicles, close to adherens junctions and desmosomes, as well as in the nucleus; co-localizes with clathrin and with N-Wasp but not with caveolin-1, and in Caco-2 cells Dab1 localizes at cell-to-cell junctions by a Ca^{2+}-dependent process. In conclusion, the results indicate that in rodent intestine a truncated Dab1 variant transmits the reelin signal and may play a role in clathrin-mediated apical endocytosis and in the control of cell-to-cell junctions assembly. A function of intestinal Dab1 variant as a nucleocytoplasmic shuttling protein is also inferred from its sequence and nuclear location.

Keywords: intestine, Dab1 isoform, endocytosis, cell-cell junctions

1. Introduction

Disabled-1 (Dab1) is a cytoplasmic adaptor protein essential for reelin control of neuronal migration and cellular layer formation in the developing brain. Through the PTB domain (phosphotyrosine-binding domain) of its N-terminal region, Dab1 binds to the cytoplasmic tail of lipoprotein receptors, including apolipoprotein E receptor 2 (ApoER2) and very low density lipoprotein receptor (VLDLR), and, upon reelin binding to these receptors, it becomes phosphorylated on tyrosine residues. Brain Dab1 (canonical Dab1) contains five highly conserved tyrosine residues (Y^{185}, Y^{198}, Y^{200}, Y^{220} and Y^{232}) capable of being phosphorylated after reelin stimulation [1]. These residues correspond to two consensus Src family kinase recognition sites (Y^{185} and Y^{198}) and two consensus Abl/Crk recognition sites (Y^{220} and Y^{232}) [2]. Some authors have observed that reelin action requires phosphorylation of at least Y^{198}, Y^{220} and Y^{232} [1,3,4] and Katyal et al. (2007) [4], proposed that Y^{185} phosphorylation plays a modifying role in Dab1 phosphorylation. However, in studies *in vivo*, Morimura and Ogawa (2009) [5] found redundancy in the two tyrosine residues of the pairs Y^{185}/Y^{198} and Y^{220}/Y^{232} so that phosphorylation of either one of the residues in each pair is sufficient for reelin signal transmission. They proposed two reelin signalling pathways, one mediated by the Y^{185}/Y^{198} phosphorylation of Dab1 and the other by phosphorylation at Y^{220}/Y^{232}. Whatever the situation, once the tyrosines are phosphorylated, Dab1 activates downstream signalling cascades that through changes in the cytoskeleton lead to the proper positioning of migrating neurons (see Gao and Godbout, 2013 for a review) [6]. A role of Dab1 in endo/exocytosis [7–9] and as a nucleocytoplasmic shuttling protein has also been reported [10,11].

Three Dab1 mRNA transcripts of 5.5, 4.0 and 1.8 kb have been identified and the 5.5 kb transcript encodes the canonical Dab1 and 5 additional variants. These 6 isoforms share the N-terminal, that contains the high conserved PTB domain, and the C-terminal domains, but some variants exclude exons containing some of the tyrosine phosphorylation sites [12]. Some observations revealed that the alternative splicing that generates the multiple Dab1 variants is developmentally regulated. Thus, in human/chicken retina, undifferentiated cells express “Dab1 early isoform” (chDab1-E) and a “late isoform” (chDab1-L) is expressed in amacrine and ganglion cells [13,14].

The small intestine also expresses Dab1 and we were the first to report: i) its expression as well as that of reelin and reelin receptors VLDLR and ApoER2 in rodent and human intestine and ii) that mice deficient in either reelin (*reeler* mutation) or Dab1 (*scrambler* mutation) have similar morphology of the villi and rates of the cell renewal processes, suggesting that Dab1 functions downstream of reelin action in the homeostasis of the crypt–villus unit [15–17]. In addition to attenuating epithelial cell renewal processes, both *reeler* and *scrambler* mutations expand the extracellular space at the level of adherens junctions and desmosomes. This alteration is not due to mislocalization of the E-cadherin and β-catenin because the mutations did not modify the cell membrane localization of these proteins [16,17]. As reelin/Dab1 signalling system affects the actin cytoskeleton in brain, changes in the dynamics of the actin cytoskeleton might explain the observed junctional alterations.

However, in spite of these observations suggesting that Dab1 transmits reelin signals, the isoform detected in mice enterocytes by Western blot has a molecular weight (approx. 63 kD) similar to the molecular weight of variant 6 [17]. Variant 6 lacks the tyrosine residues Y^{198} and Y^{220} that, according to some authors, are required for reelin action [1,3,4,12]. Alternatively, the intestinal isoform could be the canonical Dab1 (80 kD) with different degree of amino acids residues phosphorylation [18].

The purpose of the current work was to determine the Dab1 isoform/s present in the intestine, their subcellular localization and their co-localization with proteins involved in endo- and exocytosis.

A preliminary report of some of these results was published as a Meeting abstract [19].

2. Materials and methods

2.1. Materials

The antibodies used in the current study were: rabbit anti-Dab1 (Chemicon), rabbit anti-Dab1 (AbCam), rabbit anti-Dab1 (ABR), mouse anti-clathrin (BD Transduction Laboratories), mouse anti-N-Wasp (Santa Cruz), mouse anti-caveolin-1 (BD Transduction Laboratories), mouse anti-β-Actin (Sigma-Aldrich), biotin-conjugated anti-rabbit IgG (Vector), gold-conjugated anti-rabbit IgG (6 nm, Aurion), gold conjugated anti-mouse IgG (10 nm, Aurion), peroxidase-conjugated anti-rabbit IgG (Sigma-Aldrich), peroxidase-conjugated anti-mouse IgG (Sigma-Aldrich) and Alexa Fluor 488-conjugated anti-rabbit IgG (Invitrogen). Dulbecco's Modified Eagle's Medium (DMEM), fetal calf serum (FCS), penicillin and streptomycin were from Invitrogen. The anti-Dab1 antibodies used in the current study are raised against the C-terminus and hence recognise all Dab1 isoforms coded by the 5.5 kb transcript. Unless otherwise indicated the other reagents used in this study were from Sigma-Aldrich (Spain).

2.2. Biological preparations

Small intestine was obtained from 15 and 30 day-old Wistar rats and the colon from 3 month-old C57BL/6 mice. The animals were housed in a 12:12 light-dark cycle and fed *ad libitum* with normal rodent diet (Harlan Ibérica S.L.) with free access to tap water. They were humanely handled and sacrificed by a lethal intraperitoneal injection of pentobarbital (50 mg/kg) in accordance with the guidelines of the European Union Council (Directive 2010/63/UE) concerning the protection of experimental animals.

Stable human epithelial colorectal adenocarcinoma cells (Caco-2) were grown in DMEM supplemented with 20% FCS and in the presence of 100 U/ml penicillin and 100 µg/ml streptomycin at 37°C and in a 5% CO_2 atmosphere.

2.3. Isolation of intestinal epithelial and crypt cells

The small intestine was rapidly removed and washed with ice-cold saline solution. Enterocytes and crypts were sequentially isolated by a Ca^{2+}-chelation technique as previously described [20]. Briefly, 2 cm intestinal segments were incubated in a shaking water bath at 37°C for 15 min. The incubation buffer contained in mM: 96 NaCl, 27 $Na_3C_3H_5O(COO)_3$, 0.8 KH_2PO_4, 5.6 Na_2HPO_4, 1.5 KCl, 10 glucose and 0.5

dithiothreitol, pH 7.4 (buffer A). Thereafter the intestinal segments were incubated for 30 min at 37°C in buffer B containing PBS (in mM, 137 NaCl, 2.7 KCl, 10.1 Na_2HPO_4 and 1.8 KH_2PO_4 pH 7.4), 1.5 mM EDTA, 10 mM glucose and 0.5 mM dithiothreitol. Following incubation, the tissues were vortexed for 30 s to remove epithelial cells from the villi. Loosened epithelial cells were filtered through 60 µm nylon cloth and collected by centrifugation and resuspension in PBS. They constitute the enterocytes enriched fraction. The tissues were incubated for another 20 min in buffer B, vortexed for 30 s and the buffer containing epithelial cells discarded. This step is repeated for 3 times. Following a 20 minutes incubation period in buffer B, the tissues were vortexed gently for 5 min and the crypt cells collected by centrifugation and resuspension in PBS. During all the incubation periods the intestinal segments were continuously gassed with 95% O_2-5% CO_2, shaken and maintained at 37ºC. The cell enrichment of each fraction was evaluated by measuring the mRNA relative abundance of markers characteristic of enterocytes, SGLT1 and of crypt cells, Na^+-K^+-$2Cl^-$ cotransporter 1 (NKCC1). The enrichment factor in each fraction, defined as the ratio of the mRNA levels in the two compartments, was around 7.

2.4. Immunostaining at the light microscope

Immunostaining assays were performed on intact small intestine as previously [17] and in Caco-2 cells. Briefly, 5 µm thick paraffin embedded sections of small intestine, previously fixed by overnight incubation with PBS containing 4% paraformaldehyde at 4°C, were applied to adhesive-coated glass slides and permeabilized by boiling with 0.01 M sodium citrate, pH 6, during 10 min. Caco-2 cells were grown on glass coverslips for 3 days and fixed directly in methanol at −20°C for 10 min. After blocking with 5% bovine serum albumin and 3% FCS in PBS for 1 h, the intestinal sections and Caco-2 cells were incubated with the rabbit anti-Dab1 antibody (1:300 dilution) at 4ºC, overnight. Controls were carried out without primary antibody. In the intestine the anti-Dab1 antibody binding was visualized with biotin-conjugated anti-rabbit IgG secondary antibody (1:200 dilution), followed by immunoperoxidase staining using the Vectastain ABC peroxidase kit (Vector) and 3,3'-diaminobenzidine. In Caco-2 cells the antibody was visualized with FITC-conjugated anti-rabbit IgG secondary antibody (1:500 dilution) and the nuclei with Hoechst 33258 (Invitrogen). The intestinal slides were rinsed,

mounted and photographed with a Zeiss Axioskop 40 microscope equipped with a SPOT Insight V 3.5 digital camera. Coverslips containing the Caco-2 cells were washed and mounted with mounting medium (ProLong Gold, Invitrogen) and stored at 4°C. Epifluorescent images were collected with a fluorescent microscope (DMIRB, Leica) using an Apochromat 63×, 1.4 NA oil immersion objective fitted with a camera (C4742-95, Hamamatsu Photonics) and SimplePCI software (Hamamatsu Photonics).

2.5. Immunostaining at the electron microscope

Immunostaining at the electron microscope was carried out as before [20]. Segments of the small intestine obtained from 15 day-old rats were fixed in 1% glutaraldehyde, 4% formaldehyde and 0.25% picric acid in 0.1 M phosphate buffer, pH 7.4 at room temperature for 3 h. After rinsing in phosphate buffer containing 3.5% sucrose (buffered sucrose), the segments were incubated for 1 h in 0.5 M ammonium chloride in buffered sucrose. Fixed tissue was dehydrated directly into 70% ethanol and embedded in LR White resin at 50°C for 24 h using gelatine capsules. Ultrathin sections (90 nm) were mounted on nickel grids, transferred onto PBS, blocked for 15 min with 0.5% BSA diluted in PBS and incubated with the indicated primary antibody for 2 h at room temperature. The grids were rinsed, incubated for 1 h at room temperature with the appropriate gold-conjugated secondary antibody and washed with PBS-BSA (3x10 min), PBS (3x10 min) and distilled water (3x10 min). Controls were carried out without primary antibody (data not shown). Grids were stained with 2% uranyl acetate for 10 min, washed with distilled water and examined under a Zeiss Libra 120 Plus transmission electron microscope equipped with a TRS camera. The microphotographs were processed with ImageJ software version 1.46 (National Institutes for Health http://rsb.info.nih.gov/ij/ index.html) for a quantitative analysis of the distances between the immunogold particles that mark the proteins under study, following the method of Bergersen et al. (2012) [21]. A gold particle was ascribed to a morphologically identified compartment (microvilli, junctions, apical vesicles and nucleus) when the centre of the particle was located within a 30 nm distance from the compartment limiting membrane. For co-localization of proteins, the intercenter distances between gold particles were measured and the distances were sorted into bins of 45 nm. Proteins are considered to be co-localized when the intercenter distances between the gold particles is <90 nm.

The frequency distributions of gold particles distances were evaluated by the Chi-squared test. For each gold particles combination, we quantified 10 of either microvilli, junctions, apical vesicles or nucleus.

2.6. Protein dephosphorylation assays

Protein extracts obtained from rat brain and enterocytes were dephosphorylated by incubating 15 µg of protein with 15 units of calf intestinal alkaline phosphatase (AP) (New England BioLabs, M0290S), at 37ºC for 1h, according to the manufacturer´s instructions. The protein concentration in the extracts was measured by the Bradford method [22] using gamma globulin as the standard.

The number of amino acid residues dephosphorylated was evaluated by dividing the AP –induced molecular weight decrease by the phosphate group molecular weight.

2.7. Western blot assays

Protein was extracted from brain and from enterocytes or crypt cells enriched fractions obtained from 1 month-old rats. In some experiments brain and enterocytes protein extracts were dephosphorylated as indicated above. Western blot assay was carried out as previously [16]. SDS-PAGE was performed on a 7.5% polyacrylamide gel. The lysis buffer contained: 150 mM NaCl, 50 mM Tris-HCl (pH 7.4), 1 mM EDTA, 1% Triton X-100, 20 µg/ml aprotinin, 10 µg/ml leupeptin and 1 mM phenylmethylsulfonyl fluoride. For protein extraction enterocytes and crypt cells were homogenized in lysis buffer, using a polytron homogenizer, and incubated at 4ºC for 10 min on a rotating shaker, followed by centrifugation at 14,000 g for 30 min. The resultant supernatant was dissolved in the Laemmli sample buffer. A total of either 50 µg (Fig. 1A) or 15 µg (Fig. 1B) protein were loaded to each lane, electrophoresed, electrotransferred onto a nitrocellulose membrane and the immunoreactive bands were viewed using a chemiluminescence procedure (GE Healthcare Select®). Anti-β-actin antibody was used to normalize band density values. The relative abundance of the bands was quantified using the Image J program version 1.46 (National Institutes for Health, http://rsb.info.nih.gov/ij/index.html). The protein concentration in the extracts was measured by the Bradford method [22] using gamma globulin as the standard.

2*.8. Relative quantification by Real-time PCR*

Total RNA was extracted from the enterocytes and crypt cells of 1 month-old rats small intestine using RNeasy® kit (Qiagen, Hilden, Germany). RNA purity was assessed by spectrophotometry measurements of $OD_{260/280}$ and its integrity by visual inspection after electrophoresis on an agarose gel in the presence of RedSafe™ (Intron Biotechnology) nucleic acid staining. cDNA was synthesized from 1 µg of total RNA using QuantiTect® reverse transcription kit (Qiagen), as described by the manufacturer. The primers (sense CTAGGCAGAGCTCTCCATCC / antisense GACTTATATTATCACCACTGGGCTC) amplified a Dab1 fragment located in the C-terminus sequence of Dab1 and were chosen according to the murine cDNA sequences entered in Genbank and designed using PerlPrimer program v1.1.14 (Parkville, Melbourne, Victoria, Australia). Real-time PCR was performed with 10 µl SsoFast™ EvaGreen® Supermix (BioRad), 0.4 µM primers and 1 µl cDNA. Controls were carried out without cDNA. Amplification was run in a MiniOpticon™ System (BioRad) thermal cycler (95 °C /3 min; 35 cycles of 94 °C /40 s, 58 °C/ 40 s and 72 °C/ 40 s, and 72 °C /2 min). Following amplification, a melting curve analysis was done by heating the reactions from 65 to 95 °C in 1 °C intervals while monitoring fluorescence. Analysis confirmed a single PCR product at the predicted melting temperature. The cycle at which each sample crossed a fluorescence threshold, Ct, was determined and the triplicate values for each cDNA were averaged. Analyses of PCR were done using the comparative Ct method with the Gene Expression Macro software supplied by BioRad. β-Actin (sense CGGAACCGCTCATTGCC/ antisense, ACCCACACTGTGCCCATCTA) served as reference gene and was used for samples normalization.

2.9. Identification of intestinal Dab1 isoform

Intestinal Dab1 isoform was determined by reverse transcription and PCR analysis of Dab1 sequence. Total RNA, extracted from whole small intestine of 1 month-old rats and whole distal colon of 3 month-old mice, was reverse-transcribed (QuantiTect® Reverse Transcription Qiagen) and the cDNA obtained amplified by PCR. PCR was performed with MyFi™ DNA polymerase (Bioline), 0.4 µM primers and 2 µl cDNA. Controls were carried out without cDNA. Amplification was run in a MiniOpticon™ System (BioRad) thermal cycler (95 °C /1 min; 35 cycles of 95 °C /15 s, 55 °C/ 15 s and 72 °C/ 45 s, and 72 °C /5 min). The primers used were (sense / antisense):

ATGTCAACTGAGACAGAAC / CTGAGCTCCTGGTATCACCTG according to the murine cDNA sequences entered in Genbank and designed using PerlPrimer program v1.1.14 (Parkville, Melbourne, Victoria, Australia). The whole sequence of intestinal Dab1 was analysed, including the sequences of 9b+9c exons. The PCR products were electrophoresed on 2% agarose gels and visualized by RedSafe™ (Intron Biotechnology) staining. The amplified cDNAs were extracted and purified from the gel (QIAquick Gel extraction kit, Qiagen) and sequenced (AB3500 Genetic Analyzer Applied Biosystems). cDNA sequencing was performed on both strands from at least 3 independent PCR products and the resulting sequences were compared with the nucleotide sequences database from the National Center for Biotechnology Information (NCBI: http://www.ncbi.nlm.nih.gov) using BLAST program.

2.10. Calcium switch experiments

Caco-2 cells were plated over coverslips an incubated in low calcium medium containing dialysed FCS [23]. After 24 hours, the low calcium medium was replaced by normal DMEM medium and the cells incubated for different time periods. At the desired times, the medium was removed and the cells were fixed for Dab1 immunostaining using the rabbit anti-Dab1 antibody (Chemicon; 1:300 dilution).

2.11. Statistical analysis

Data are presented as mean ± SEM. Comparisons between different experimental groups were evaluated by the Student's t-test ($p<0.05$). For quantitative immunogold analysis (Figs. 4-7) Chi-squared test was used. Differences were set to be significant for $p<0.01$.

3. Results

3.1. Dab1 expression along the crypt-villus axis

Previous Western blot assays carried out in our laboratory [17], revealed that the anti-Dab1 antibody recognizes in mice enterocytes three polypeptides bands and that the band absent in the *scrambler* mice was that of 63 kD, indicating that this polypeptide band corresponds to Dab1. To find out whether the crypt cells express the same Dab1 isoform as enterocytes, Western blot assays were performed with protein extracts from crypt and villus cells of rat. The results (Fig. 1A) reveal that the anti-Dab1 antibody recognizes the same polypeptides bands in both enterocytes and crypt cells and that the intensity of the 63 kD band is similar in the two types of epithelial cells, indicating that they express the same Dab1 isoform.

Dab1 mRNA relative levels, determined by Real-time PCR, were also of similar magnitude in enterocytes (2.6 ± 0.6, n=9) and crypt cells (2.5 ± 0.5, n=10).

These observations indicate that the epithelial cells of rodent small intestine express only one Dab1 isoform.

3.2. Identification of Dab1 isoform in rodent small and large intestine

To determine whether the Dab1 isoform present in rodent intestine corresponds to any of the Dab1 isoform described so far, intestinal Dab1 was amplified from cDNAs generated from rat small intestine. The PCR fragments sequenced encoded a Dab1 isoform 100% identical to Dab1 variant 6 (Fig. 2). The isoform i) has a total number of amino acids of 552, which corresponds to a MW of approximately 63 kD; ii) excludes exons 7 (containing tyrosine Y^{198}) and 8 (containing tyrosines Y^{200} and Y^{220}); iii) includes exons 9b and 9c that leads to a 99 nucleotide insertion between exons 9 and 10; iv) contains two leucine-rich nuclear export signals (NESs) and a bipartite nuclear localization signal (NLS1); and v) harbours two lysines at K^{67} and K^{69} in exon 3. Since exons 7 and 8 are excluded, the isoform carries only the tyrosine residues Y^{185} and Y^{232}.

As in previous studies we used mouse distal colon to determine the role of reelin/Dab1 system, we also determined the isoform expressed by this tissue and found that it is variant 6.

Though Dab1 variant 6 and canonical Dab1 have the same number of amino acids, they differ in their apparent molecular weight, 63 kD *vs*. 80 kD, respectively. To determine whether the difference results from differences in the phosphorylation degree, Western blot assays were performed with brain and enterocytes protein extracts with or without alkaline phosphatase treatment. Fig. 1B shows that dephosphorylation reduces the size of canonical Dab1 and that of variant 6 by approximately 4.00 and 2.90 kD, respectively, which corresponds to approximately 50 and 37 phosphate groups, respectively. The alkaline phosphatase treatment completely dephosphorylated the Dab1 isoforms tested because a single dephosphorylated polypeptide band is observed for each isoform, indicating that canonical Dab1 has around 50 phosphorylated amino acid residues and 37 the Dab1 variant 6. Fig. 1B also shows that the dephosporylated isoforms still have different molecular weights, approximately 76 kD and 60 kD, respectively, indicating that the differences cannot be attributed exclusively to phosphorylation.

3.3. Cell localization of Dab1 and its co-localization with N-Wasp, clathrin and caveolin-1

The localization of Dab1 in the intact rat small intestine was first determined by immunohistochemistry combined with light microscopy. As previously reported [15], the specific signal produced by the anti-Dab1 antibody is observed throughout the crypt-villus axis and in the villus the signal is detected at the apical and lateral membranes and at the cytosol (Fig. 3).

The subcellular localization of Dab1 and its co-localization with proteins forming endocytic membrane invaginations, such as caveolin-1 and clathrin, and with proteins that control actin cytoskeleton, such as Neural Wiskott-Aldrich Syndrome Protein (N-Wasp), were examined by single or double immunogold electron microscopy. A gold particle was ascribed to a morphologically defined compartment (microvilli, junctions, apical vesicles and nucleus) when the centre of the particle was located within a 30 nm distance from the compartment limiting membrane. Figure 4 shows that the immunogold particles labelling Dab1 are at less than 30 nm distance of membrane invaginations, apical vesicles, endosomes, nucleus and close to adherens junctions and desmosomes, indicating that the protein is located in those compartments. When clathrin and Dab1 were immunostained simultaneously, both proteins are detected at microvilli, terminal

web, apical vesicles and junctions (Fig. 5A) and the majority of intercenter distances between the gold particles marking Dab1 and clathrin are lower than 90 nm (Fig. 5B), indicating co-localization of the two proteins. Dab1 also co-localizes with clathrin at the nucleus (Fig. 5A). Co-localization of Dab1 and N-Wasp was only seen at vesicles (Fig. 6). In all the places examined, the distances between the gold particles marking Dab1 and caveolin-1 are greater than 150 nm ruling out their co-localization (see Fig.7). Immunoreactive signal was not seen in the absence of the primary antibody (data not shown). The observations suggest a role for Dab1 in clathrin-mediated endocytosis.

3.4. Effect of extracellular Ca^{2+} on Dab1 distribution in Caco-2 cells.

As the immunolocalization studies revealed Dab1 localization close to adherens junctions and desmosomes, we next evaluated: i) whether Dab1 is related to the establishment of cell-cell junctions and ii) the effect of extracellular Ca^{2+} on the subcellular Dab1 localization. In these experiments we used Caco-2 cells. Figure 8A shows that when the cells were incubated in normal medium, the anti-Dab1 antibody stained cell-to-cell contacts. When the cells were placed in low calcium medium, Dab1 is only detected in the cytosol, but following Ca^{2+} addition to the extracellular medium, Dab1 migrates from the cytosol to the plasma membrane (Fig. 8B). These observations indicate that Dab1 recruitment to the lateral membrane is triggered by calcium-induced cell-cell adhesion.

4. Discussion

Previous observations suggested that reelin actions on the intestinal epithelium are mediated by Dab1 [17] and the current observations reveal that the Dab1 isoform expressed in rodent small and large intestine is the variant 6, which excludes exons 7 (Y^{198}) and 8 (Y^{200}, Y^{220}) but includes exons 9b and 9c [12]. As the canonical Dab1, the intestinal isoform has 2 nuclear export signals (NES), a nuclear localization signal (NLS1) and two lysines at K^{67} and K^{69} that might be part of an unidentified NLS2 [24]. In spite of having Dab1 variant 6 and canonical Dab1 the same number of amino acids, they differ in their apparent molecular weight. Dephosphorylation reduces the molecular weight of both isoforms and the number of amino acid residues dephosporylated agrees with those expected from their amino acid sequence [25]. The molecular weight difference, however, is not eliminated by dephosphorylation, discarding the previously suggested variations in the degree of phosphorylation as the sole cause for the molecular weight differences [18]. Other post-translational modifications might contribute to the observed molecular weight difference, such as variations in protein glycosylation

From the functional point of view, the main difference between the canonical Dab1 and variant 6 is that the former contains the complete set of tyrosine phosphorylation sites whereas the intestinal variant misses Y^{198}, Y^{200} and Y^{220}. Therefore, it lacks two (Y^{198} and Y^{220}) of the three tyrosine phosphorylation sites (Y^{198}, Y^{220} and Y^{232}) considered by some authors essential for fully response to reelin signal [1,3,4,12]. According to Morimura and Ogawa (2009) [5], however, the variant 6 could transmit the reelin signal as it has one of the tyrosine residues of each pair (Y^{185} in the pair Y^{185}/Y^{198} and Y^{232} in Y^{220}/Y^{232}), that once phosphorylated would activate the two reelin signalling pathways proposed by these authors. Whether or not the intestinal isoform assembles the set of downstream signalling complexes triggered by the Dab1 containing the five tyrosine residues, it does transmit the reelin signal to downstream cytosolic components. Thus, previous observations showed that: i) as in the brain, the *reeler* mutation increases intestinal Dab1 protein abundance without affecting Dab1 mRNA levels [17], a finding interpreted as the requirement of reelin for Dab1 degradation [25, 26] and ii) both, *scrambler* [17] and *reeler* [16] mutations induce extremely similar changes in the morphology of the villi, the dynamics of the crypt–villus axis and the structure of

adherens junctions and desmosomes. The presence of either canonical Dab1 or truncated Dab1 in a tissue might be related to the contribution of reelin signalling to tissue homeostasis. Reelin is crucial for brain development and the brain expresses the Dab1 isoform that contains the 5 tyrosine phosphorylation sites. In the intestine, reelin signalling appears to be a redundant control mechanism because, although it is needed for the normal epithelium phenotype, its absence does not prevent epithelium development and function [16]. However, under non-physiological circumstances, such as colitis and colon cancer, the reelin system becomes more relevant as its absence increases the susceptibility of mice to develop such pathologies [28–30]. Another example of the functional complexity of Dab1 isoforms in specific tissues is the pig liver, which expresses the Dab1 variant 4 that only carries Y^{185} and Y^{232} [31]. It seems, therefore, that different Dab1 variants serve different signalling functions in different tissues.

The information on the downstream pathways to which Dab1 transmits reelin signals in the brain is profuse but the affected pathways in non-neural tissues remain unrevealed. In the brain, phosphorylated Dab1 activates proteins that modulate cytoskeletal dynamics (see Gao and Godbout, 2013 for a review) [6]. Our previous studies [16,17], showing that *reeler* or *scrambler*-induced expansion of adherens junctions and desmosomes was not due to mislocation of E-cadherin and β-catenin, suggest that reelin/Dab1 system might regulate these junctions via the cytoskeleton. Some of the current observations may support this point of view. Thus, Dab1 localizes in the intestine at enterocytes lateral membranes and close to adherens junctions and desmosomes. In addition, Dab1 is recruited to cell-to-cell contacts in Caco-2 cells, a process triggered by calcium. Dab1 might be recruited to the membrane through its PTB domain that exhibits a subdomain that binds to membrane phosphoinositides [32]. Though membrane Dab1 recruitment is reelin-independent, because reelin was absent from the incubation medium and Caco-2 cells lack reelin [15], Dab1 posterior action could be reelin-dependent. In this respect, recently, it has been reported that reelin transiently promotes N-cadherin-dependent neuronal adhesion during mouse cortical development [33].

The subcellular location of Dab1 at apical membrane pits and apical vesicles and

its co-localization with clathrin, but not with caveolin-1, indicates a role for Dab1 in clathrin-mediated endocytosis. Dab1 co-localizes with the actin polymerization activator N-Wasp at cytosolic vesicles, suggesting a role for Dab1 in endo/exocytic processes via actin cytoskeleton. In this respect, involvement of Dab1 in the actin cytoskeleton regulation through direct binding of Dab1 with N-Wasp [34] and in endocytosis mediated by low density lipoprotein receptors, such as megalin, LDLR and VLDLR [7–9], has been reported. Whether the involvement of Dab1 in these processes is reelin-dependent requires further investigation.

The intestinal Dab1 could also function as a nucleocytoplasmic shuttling protein because it has nuclear localization/export signals (NLS and NESs) and it also localizes at the nucleus. These observations agree with those of Martin-Lopez et al. (2011) [11] in the olfactory bulb and with those of Honda and Nakajima (2006) [10] in cerebral neurons from embryos. The observed nuclear localization of Dab1 indicates that the absence of Y^{198}, Y^{200} and Y^{220} does not prevent its entry into the nucleus and hence its nucleocytoplasmic shuttling. Honda and Nakajima (2006) [10] suggested that Dab1 nucleocytoplasmic shuttling is independent of tyrosine phosphorylation.

It was a surprise to detect clathrin in the nucleus. However, Enari et al. (2006) [35] found that the monomeric clathrin heavy chain translocates into the nucleus bound to the tumour suppressor protein p53. Therefore the Dab1/clathrin detected in the enterocytes nucleus could represent Dab1 binding to monomeric clathrin heavy chain. Alternatively, the nuclear co-localization of Dab1 with clathrin might not be such, but instead be a co-localization of Dab1 with nucleoporins. Thus, the anti-clathrin antibody used recognizes a clathrin region that includes the β-propeller sequence of nucleoporins [36] and hence the antibody might be recognising nucleoporins instead of clathrin. Co-localization of Dab1 with nucleoporin would suggest that Dab1 enters the nucleus by binding to proteins within the nuclear pore complex itself.

In summary, rodent intestine expresses the Dab1 variant 6 that carries only two of the five tyrosine residues present in the canonical Dab1. Dab1 variant 6 localizes with clathrin at apical endocytic vesicles, cell-to-cell junctions and nucleus, suggesting a function in clathrin-mediated endocytosis and as nucleocytoplasmic shuttling protein. Dab1 assembly in Caco-2 cells can be manipulated by extracellular calcium that would

suggest that the truncated Dab1 variant could be involved in Dab1 regulation of cell-cell adhesion.

Acknowledgements

This work was supported by a grant from the Junta de Andalucía (CTS 5884), by fellowships from the Spanish “Ministerio de Educación y Ciencia” (AP2007-04201) and from The European Molecular Biology Organization (EMBO; ASTF45-2012) to M.D. Vázquez-Carretero. Electronmicroscopy images were obtained in the Centro de Investigación, Tecnología e Innovación, Universidad de Sevilla. We thank Francisco Ramos from the Department of Microbiology of the University of Seville for his technical advice.

Figure legends

Fig.1. Expression of Dab1 in enterocytes, crypt cells and brain. Western blot of Dab1 was performed on brain and on enterocytes and crypt cells enriched fractions obtained from small intestine of 1 month-old rats. A. Proteins extracts from enterocytes and crypts enriched fractions. 50 µg protein per lane were loaded. The blot was probed with anti-Dab1 antibody (Chemicon, 1:2,000 dilution). β-Actin was used as a reference protein. Histograms represent the relative abundance of Dab1 in the intestinal extracts. B. Brain and enterocytes protein extracts with and without alkaline phosphatase (AP) treatment. 15 µg protein per lane were loaded. The blot was probed with anti-Dab1 antibody (ABR, 1:4,000 dilution). The values represent means ± SEM. Four animals were used. Student's t-test revealed no effect of the type of epithelial cell on Dab1 protein abundance.

Fig. 2. Schematic representation of rat intestine Dab1 variant. Canonical and intestinal Dab1 exons and the amino acid sequence of NLS (nuclear localization signal), NES (nuclear export signal) and the critical tyrosine phosphorylation sites are shown. The exons are not drawn to scale.

Fig. 3. Immunolocalization of Dab1 at the light microscope in the small intestine. 1 month-old rats were used. 5 µm intestinal paraffin-embedded sections were incubated with anti-Dab1 antibody (Chemicon, 1:300 dilution). The photographs are representative of three different assays. Scale bars represent 100 µm and those of the inserts 25 µm. Controls were carried out without primary antibody.

Fig. 4. Immunolocalization of Dab1 in the epithelium of rat small intestine by electron microscopy. The age of the rats was 15 days. GL: giant lysosome, J: junction, MV: microvilli, AV: apical vesicles, LE: late endosomes, EE: early endosomes, TJ: tight junction, AJ: adherens junction, D: desmosome, N: nucleus. A. Electron microphotographs of the epithelial cells. The area within the square is that shown in B. Scale bar represents 1,000 nm. B. Immunogold labelling of Dab1. The dilution of the anti-Dab1 antibody (AbCam) was 1:50. Immunogold labelling of Dab1 (6 nm) is indicated by arrows. The photographs are representative of three different assays. Scale bars represent 100 nm. C. Histograms represent the frequency of gold particles

distribution. The distances from the particles and the closer limiting cell structure membrane were sorted into bins of 15 nm. The Chi-squared test ($p<0.01$) showed significant localization for Dab1 in all the compartments studied. For each cluster, the quantifications were done in 10 either vesicles, endosomes, adherens junctions or desmosomes.

Fig. 5. Co-localization of Dab1 and clathrin at the apical domain of rat small intestine epithelium by electron microscopy. The age of the rats was 15 days. A. Electron microphotographs of an enterocyte. Immunogold labelling of Dab1 (6 nm) is indicated by arrows and that of clathrin (10 nm) by arrowheads. The dilution of the anti-Dab1 antibody (AbCam) was 1:5 and that of the anti-clathrin antibody (BD) was 1:1. MV: microvilli, TW: terminal web, V: vesicles, D: desmosome, ER: endocytic reticulum, N: nucleus. The photographs are representative of three different assays. Scale bar represents 100 nm. B. Histograms represent the frequency of gold particles distribution. Intercenter distances between gold particles were sorted into bins of 45 nm. The Chi-squared test ($p<0.01$) showed significant co-localization for Dab1 and clathrin in all the compartments studied. For each cluster, the quantifications were done in 10 either microvilli, vesicles, nucleus, junctions or terminal web area.

Fig. 6. Co-localization of Dab1 and N-Wasp at the apical domain of rat small intestine epithelium by electron microscopy. The dilution of the anti-Dab1 antibody (AbCam) was 1:5 and that of the anti-N-Wasp antibody (Santa Cruz) was 1:2. Immunogold Dab1 labelling (6 nm) is indicated by arrows and that of N-Wasp (10 nm) by arrowheads. The Chi-squared test ($p<0.01$) showed that gold labelling distribution is significantly different from random in the studied compartments. Scale bar represents 100 nm. See Fig. 5 for other details. AJ: adherens junction.

Fig. 7. Co-localization of Dab1 and caveolin-1 at the apical domain of rat small intestine epithelium by electron microscopy. The dilution of the anti-Dab1 antibody (AbCam) was 1:5 and that of the anti-caveolin-1 antibody (BD) was 1:1. Immunogold Dab1 labelling (6 nm) is indicated by arrows and that of caveolin-1 (10 nm) by arrowheads. The Chi-squared test ($p<0.01$) showed that gold labelling distribution is not significantly different

from random in both studied compartments. Scale bar represents 100 nm. See Fig. 5 for other details. AJ: adherens junction.

Fig. 8. Immunolocalization of Dab1 in Caco-2 cells at the fluorescence microscope. A. Caco-2 cells were plated in normal medium. B. Cells were plated in low calcium medium. After 24 hours the low calcium medium was replaced by normal DMEM medium and, at the desired times, the medium was removed and the cells fixed for Dab1 immunostaining using the rabbit anti-Dab1 antibody (Chemicon, 1:300 dilution). Nuclei were visualized with Hoechst. Controls were carried out without primary antibody. Scale bars represent 50 µm.

References

[1] L. Keshvara, D. Benhayon, S. Magdaleno, T. Curran, Identification of Reelin-induced Sites of Tyrosyl Phosphorylation on Disabled 1, J. Biol. Chem. 276 (2001) 16008–16014. doi:10.1074/jbc.M101422200.

[2] S. Zhou, S.E. Shoelson, M. Chaudhuri, G. Gish, T. Pawson, W.G. Haser, F. King, T. Roberts, S. Ratnofsky, R.J. Lechleider, B.G. Neel, R.B. Birge, J.E. Fajardo, M.M. Chou, H. Hanafusa, B. Schaffhausen, L.C. Cantley, SH2 domains recognize specific phosphopeptide sequences, Cell. 72 (1993) 767–778. doi:10.1016/0092-8674(93)90404-E.

[3] B.A. Ballif, L. Arnaud, W.T. Arthur, D. Guris, A. Imamoto, J.A. Cooper, Activation of a Dab1/CrkL/C3G/Rap1 pathway in Reelin-stimulated neurons, Curr. Biol. 14 (2004) 606–610. doi:10.1016/j.cub.2004.03.038.

[4] S. Katyal, Z. Gao, E. Monckton, D. Glubrecht, R. Godbout, Hierarchical Disabled-1 Tyrosine Phosphorylation in Src family Kinase Activation and Neurite Formation, J. Mol. Biol. 368 (2007) 349–364. doi:10.1016/j.jmb.2007.01.068.

[5] T. Morimura, M. Ogawa, Relative importance of the tyrosine phosphorylation sites of Disabled-1 to the transmission of Reelin signaling, Brain Res. 1304 (2009) 26–37. doi:10.1016/j.brainres.2009.09.087.

[6] Z. Gao, R. Godbout, Reelin-Disabled-1 signaling in neuronal migration: Splicing takes the stage, Cell. Mol. Life Sci. 70 (2013) 2319–2329. doi:10.1007/s00018-012-1171-6.

[7] M. Gotthardt, M. Trommsdorff, M.F. Nevitt, J. Shelton, J.A. Richardson, W. Stockinger, J. Nimpf, J. Herz, Interactions of the low density lipoprotein receptor gene family with cytosolic adaptor and scaffold proteins suggest diverse biological functions in cellular communication and signal transduction, J. Biol. Chem. 275 (2000) 25616–25624. doi:10.1074/jbc.M000955200.

[8] T. Morimura, M. Hattori, M. Ogawa, K. Mikoshiba, Disabled1 regulates the intracellular trafficking of reelin receptors, J. Biol. Chem. 280 (2005) 16901–16908. doi:10.1074/jbc.M409048200.

[9] A. Bento-Abreu, A. Velasco, E. Polo-Hernández, C. Lillo, R. Kozyraki, A. Tabernero, J.M. Medina, Albumin endocytosis via megalin in astrocytes is caveola- and Dab-1 dependent and is required for the synthesis of the neurotrophic factor oleic acid, J. Neurochem. 111 (2009) 49–60. doi:10.1111/j.1471-4159.2009.06304.x.

[10] T. Honda, K. Nakajima, Mouse disabled1 (DAB1) is a nucleocytoplasmic shuttling protein, J. Biol. Chem. 281 (2006) 38951–38965. doi:10.1074/jbc.M609061200.

[11] E. Martín-López, A. Blanchart, J.A. de Carlos, L. López-Mascaraque, Dab1 (disable homolog-1) reelin adaptor protein is overexpressed in the olfactory bulb at early postnatal stages, PLoS One. 6 (2011). doi:10.1371/journal.pone.0026673.

[12] Z. Gao, H.Y. Poon, L. Li, X. Li, E. Palmesino, D.D. Glubrecht, K. Colwill, I. Dutta, A. Kania, T. Pawson, R. Godbout, Splice-mediated motif switching regulates disabled-1 phosphorylation and SH2 domain interactions., Mol. Cell. Biol. 32 (2012) 2794–808. doi:10.1128/MCB.00570-12.

[13] S. Katyal, R. Godbout, Alternative splicing modulates Disabled-1 (Dab1) function in the developing chick retina., EMBO J. 23 (2004) 1878–1888. doi:10.1038/sj.emboj.7600185.

[14] S. Katyal, D.D. Glubrecht, L. Li, Z. Gao, R. Godbout, Disabled-1 alternative splicing in human fetal retina and neural tumors, PLoS One. 6 (2011). doi:10.1371/journal.pone.0028579.

[15] P. García-Miranda, M.J. Peral, A.A. Ilundain, Rat small intestine expresses the reelin-Disabled-1 signalling pathway., Exp. Physiol. 95 (2010) 498–507. doi:10.1113/expphysiol.2009.050682.

[16] P. García-Miranda, M.D. Vázquez-Carretero, P. Sesma, M.J. Peral, A.A. Ilundain, Reelin is involved in the crypt-villus unit homeostasis., Tissue Eng. Part A. 19 (2013) 188–98. doi:10.1089/ten.TEA.2012.0050.

[17] M.D. Vázquez-Carretero, P. García-Miranda, M.L. Calonge, M.J. Peral, A.A. Ilundain, Dab1 and reelin participate in a common signal pathway that controls intestinal crypt/villus unit dynamics., Biol. Cell. 106 (2014) 83–96. doi:10.1111/boc.201300078.

[18] B.W. Howell, F.B. Gertler, J.A. Cooper, Mouse disabled (mDab1): A Src binding protein implicated in neuronal development, EMBO J. 16 (1997) 121–132. doi:10.1093/emboj/16.1.121.

[19] M.D. Vazquez-Carretero, P. García-Miranda, M.L. Calonge, E. Calvo, J.A. López, F. Romero, M.J. Peral, A. a Ilundáin, Disabled-1 protein in the intestine, Genes Nutr. 6 (2012) S75.

[20] M.D. Vázquez-Carretero, M. Palomo, P. García-Miranda, I. Sánchez-Aguayo, M.J. Peral, M.L. Calonge, A. a Ilundain, Dab2, megalin, cubilin and amnionless receptor complex might mediate intestinal endocytosis in the suckling rat., J. Cell. Biochem. 115 (2014) 510–22. doi:10.1002/jcb.24685.

[21] L.H. Bergersen, C. Morland, L. Ormel, J.E. Rinholm, M. Larsson, J.F.H. Wold, A.T. Røe, A. Stranna, M. Santello, D. Bouvier, O.P. Ottersen, A. Volterra, V. Gundersen, Immunogold detection of L-glutamate and D-serine in small synaptic-like microvesicles in adult hippocampal astrocytes, Cereb. Cortex. 22 (2012) 1690–1697. doi:10.1093/cercor/bhr254.

[22] M.M. Bradford, A rapid and sensitive method for the quantiWcation of microgram quantities of protein utilizing the principle of protein– dye binding, Anal. Biochem. 72 (1976) 248–254.

doi:10.1016/0003-2697(76)90527-3.

[23] S.J. Terry, C. Zihni, A. Elbediwy, E. Vitiello, I. V. Leefa Chong San, M.S. Balda, K. Matter, Spatially restricted activation of RhoA signalling at epithelial junctions by p114RhoGEF drives junction formation and morphogenesis, Nat. Cell Biol. 13 (2011) 159–166. doi:10.1038/ncb2156.

[24] T. Honda, K. Nakajima, Proper level of cytosolic disabled-1, which is regulated by dual nuclear translocation pathways, is important for cortical neuronal migration, Cereb. Cortex. 26 (2016) 3219–3236. doi:10.1093/cercor/bhv162.

[25] N. Blom, S. Gammeltoft, S. Brunak, Sequence and structure-based prediction of eukaryotic protein phosphorylation sites, J. Mol. Biol. 294 (1999) 1351–1362. doi:10.1006/jmbi.1999.3310.

[26] L. Arnaud, B.A. Ballif, E. Förster, J.A. Cooper, Fyn tyrosine kinase is a critical regulator of Disabled-1 during brain development, Curr. Biol. 13 (2003) 9–17. doi:10.1016/S0960-9822(02)01397-0.

[27] H.H. Bock, Y. Jossin, P. May, O. Bergner, J. Herz, Apolipoprotein E receptors are required for reelin-induced proteasomal degradation of the neuronal adaptor protein disabled-1, J. Biol. Chem. 279 (2004) 33471–33479. doi:10.1074/jbc.M401770200.

[28] J.M. Serrano-Morales, M.D. Vazquez-Carretero, M.J. Peral, A.A. Ilundain, P. Garcia-Miranda, Reelin-Dab1 signaling system in human colorectal cancer, Mol Carcinog. (2016). doi:10.1002/mc.22527.

[29] A.E. Carvajal, J.M. Serrano-Morales, M.D. Vázquez-Carretero, P. García-Miranda, M.L. Calonge, M.J. Peral, A.A. Ilundain, Reelin protects from colon pathology by maintaining the intestinal barrier integrity and repressing tumorigenic genes, Biochim. Biophys. Acta - Mol. Basis Dis. 1863 (2017) 2126–2134. doi:10.1016/j.bbadis.2017.05.026.

[30] A.E. Carvajal, M.D. Vazquez-Carretero, P. Garcia-Miranda, M.J. Peral, M.L. Calonge, A.A. Ilundain, Reelin expression is up-regulated in mice colon in response to acute colitis and provides resistance against colitis., Biochim. Biophys. Acta. 1863 (2017) 462–473. doi:10.1016/j.bbadis.2016.11.028.

[31] H. Long, H.H. Bock, T. Lei, X. Chai, J. Yuan, J. Herz, M. Frotscher, Z. Yang, Identification of alternatively spliced Dab1 and Fyn isoforms in pig, BMC Neurosci. 12 (2011) 17. doi:10.1186/1471-2202-12-17.

[32] Y. Huang, V. Shah, T. Liu, L. Keshvara, Signaling through Disabled 1 requires phosphoinositide binding, Biochem. Biophys. Res. Commun. 331 (2005) 1460–1468. doi:10.1016/j.bbrc.2005.04.064.

[33] Y. Matsunaga, M. Noda, H. Murakawa, K. Hayashi, A. Nagasaka, S. Inoue, T. Miyata, T. Miura, K. Kubo, K. Nakajima, Reelin transiently promotes N-cadherin–dependent neuronal adhesion during mouse cortical development, Proc. Natl. Acad. Sci. 114 (2017) 2048–2053. doi:10.1073/pnas.1615215114.

[34] S. Suetsugu, T. Tezuka, T. Morimura, M. Hattori, K. Mikoshiba, T. Yamamoto, T. Takenawa, Regulation of actin cytoskeleton by mDab1 through N-WASP and ubiquitination of mDab1, Biochem J. 384 (2004) 1–8. doi:10.1042/BJ20041103.

[35] M. Enari, K. Ohmori, I. Kitabayashi, Y. Taya, Requirement of clathrin heavy chain for p53-mediated transcription, Genes Dev. 20 (2006) 1087–1099. doi:10.1101/gad.1381906.

[36] E. ter Haar, S.C. Harrison, T. Kirchhausen, Peptide-in-groove interactions link target proteins to the beta-propeller of clathrin., Proc. Natl. Acad. Sci. U. S. A. 97 (2000) 1096–100. doi:10.1073/pnas.97.3.1096.

Highlights:

Rodent intestine expresses a truncated Dab1 not regulated by cell differentiation

Dab1 localizes at the enterocytes cell membrane, cytosol and nucleus

Dab1 localizes at cell-cell junctions, in Caco2 this localization is Ca^{2+}-dependent

Intestinal Dab1 co-localizes with clathrin and with N-Wasp at apical vesicles

Intestinal Dab1 may function in endocytosis, cell-cell adhesion and nucleus processes

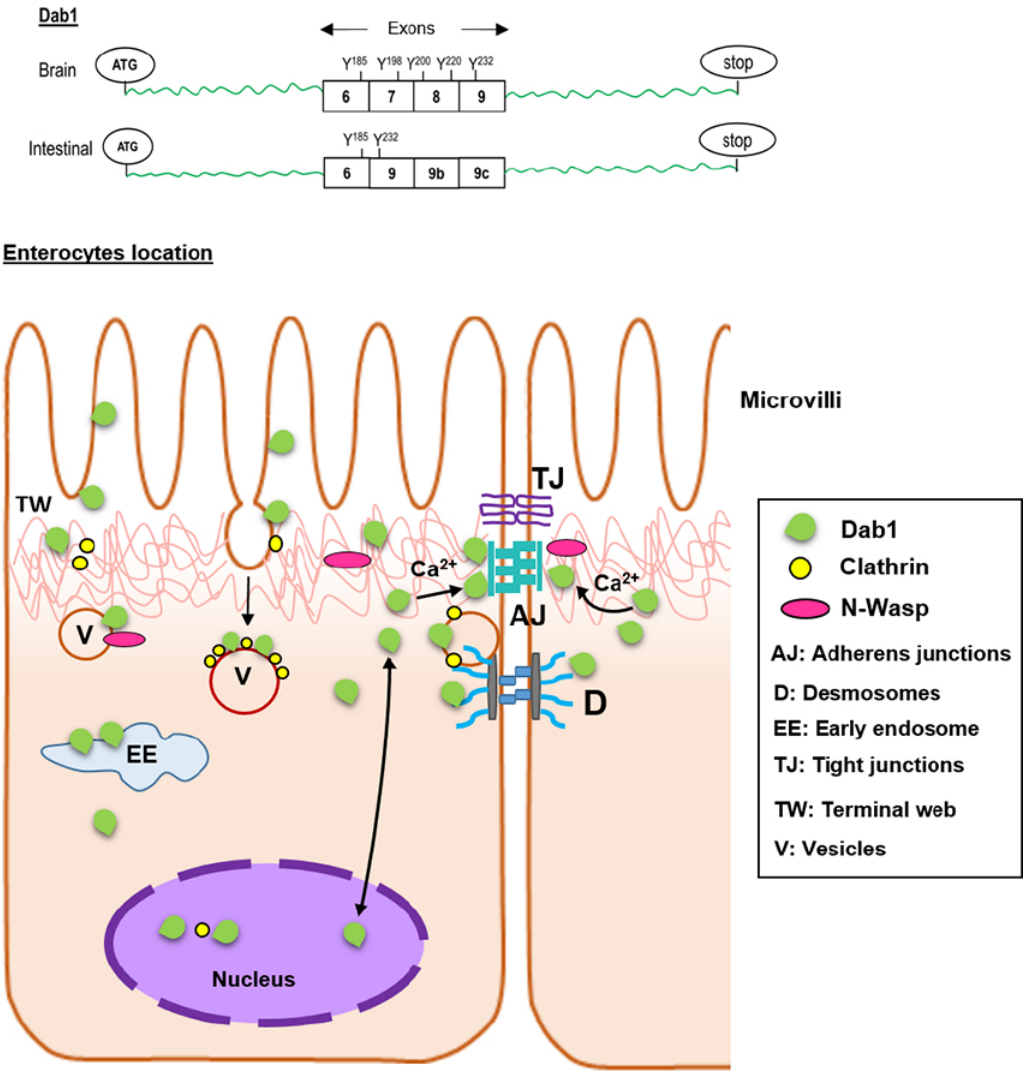

Graphics Abstract

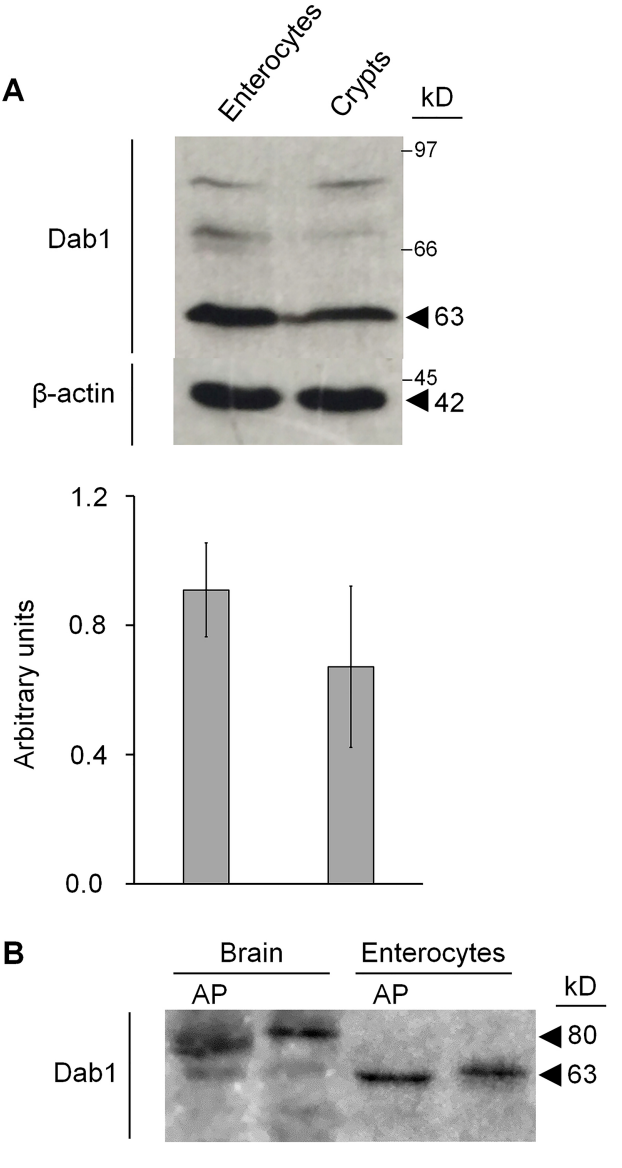
A
Enterocytes
Crypts
kD
97
66
63
45
42
Dab1
β-actin
1.2
0.8
0.4
0.0
Arbitrary units
B
Brain
Enterocytes
AP
AP
kD
80
63
Dab1

Figure 1

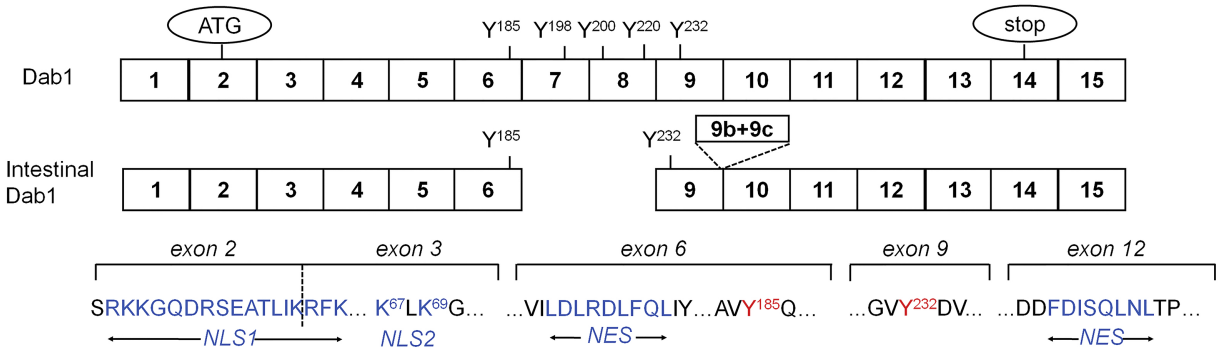
ATG
Y185 Y198 Y200 Y220 Y232
stop
Dab1
1 2 3 4 5 6 7 8 9 10 11 12 13 14 15
Y185
Y232
9b+9c
Intestinal Dab1
1 2 3 4 5 6
9 10 11 12 13 14 15
exon 2
exon 3
exon 6
exon 9
exon 12
SRKKGQDRSEATLIKRFK… K67LK69G…
…VILDLRDLFQLIY…AVY185Q…
…GVY232DV…
…DDFDISQLNLTP…
NLS1
NLS2
NES
NES

Figure 2

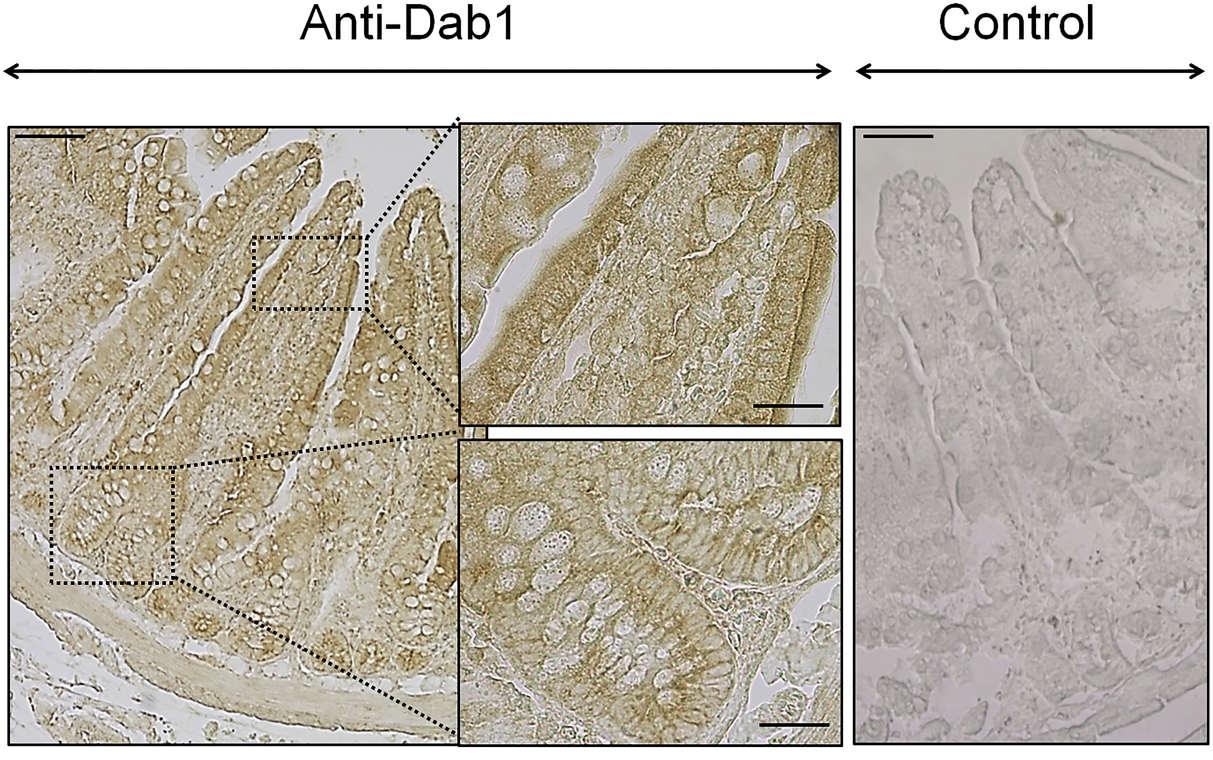

Figure 3

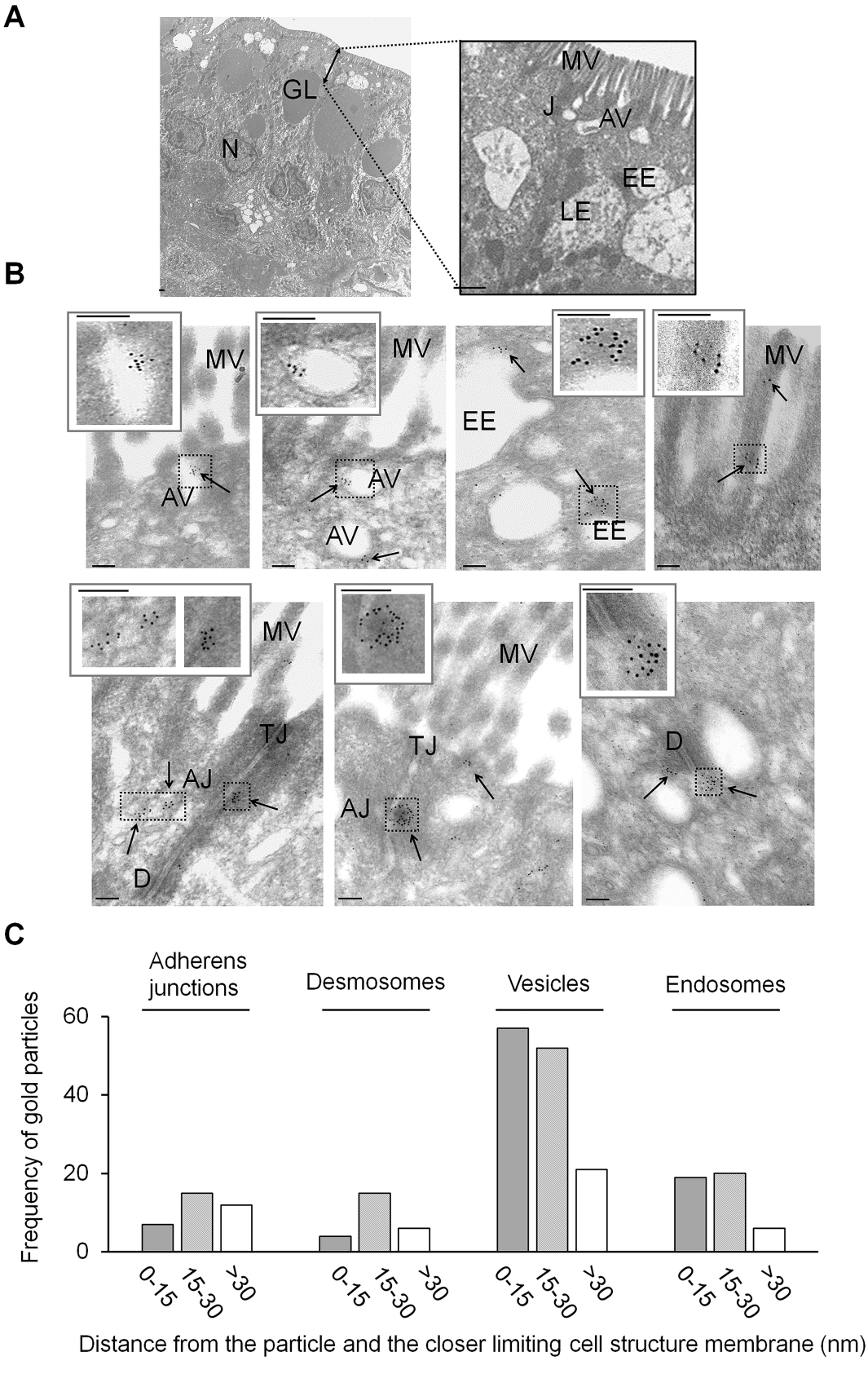
A
GL
N
MV
J
AV
EE
LE
B
MV
AV
EE
TJ
AJ
D
C
Adherens junctions
Desmosomes
Vesicles
Endosomes
Frequency of gold particles
60
40
20
0
0-15
15-30
>30
Distance from the particle and the closer limiting cell structure membrane (nm)

Figure 4

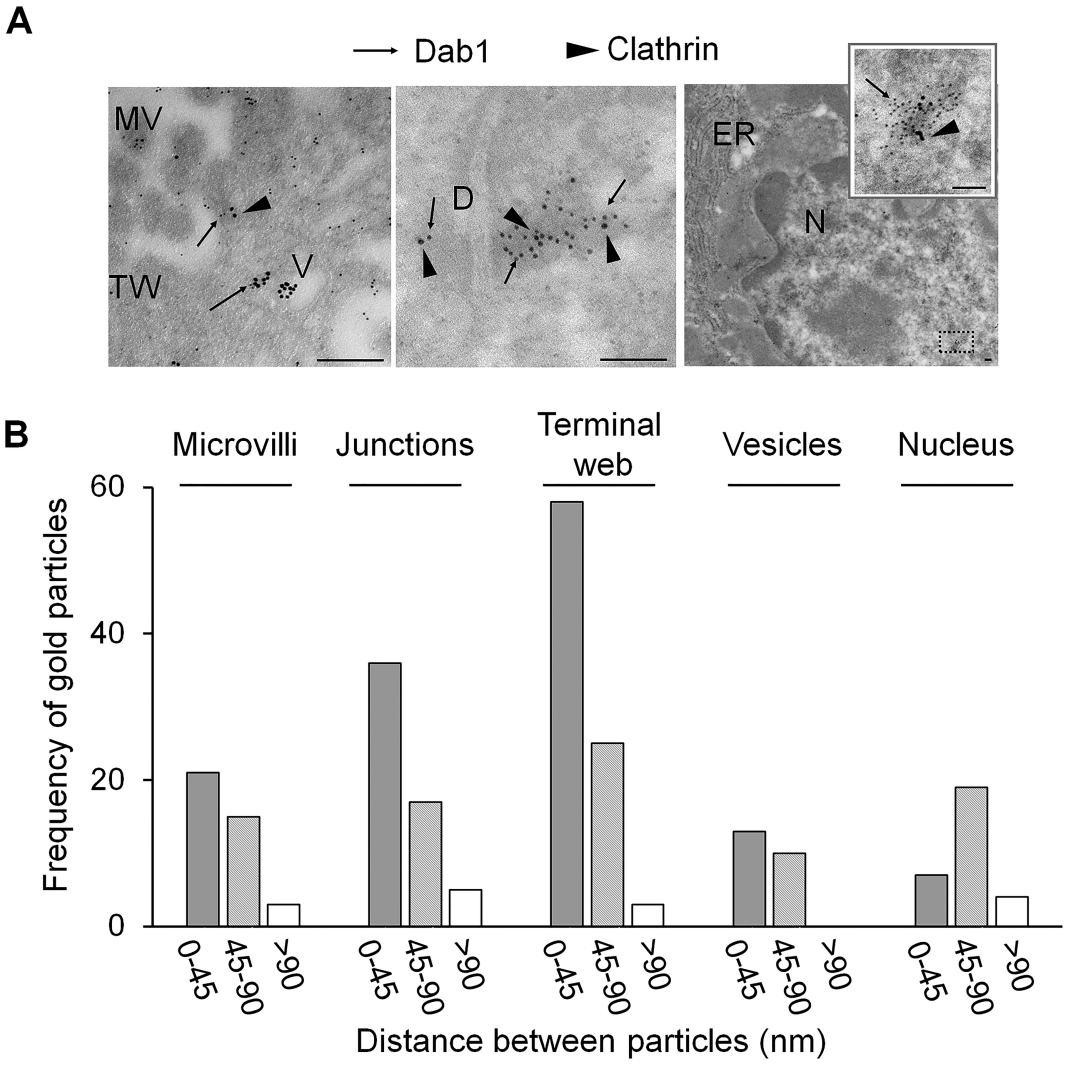
A
Dab1
Clathrin
MV
TW
V
D
ER
N
B
Microvilli
Junctions
Terminal web
Vesicles
Nucleus
Frequency of gold particles
60
40
20
0
0-45
45-90
>90
Distance between particles (nm)

Figure 5

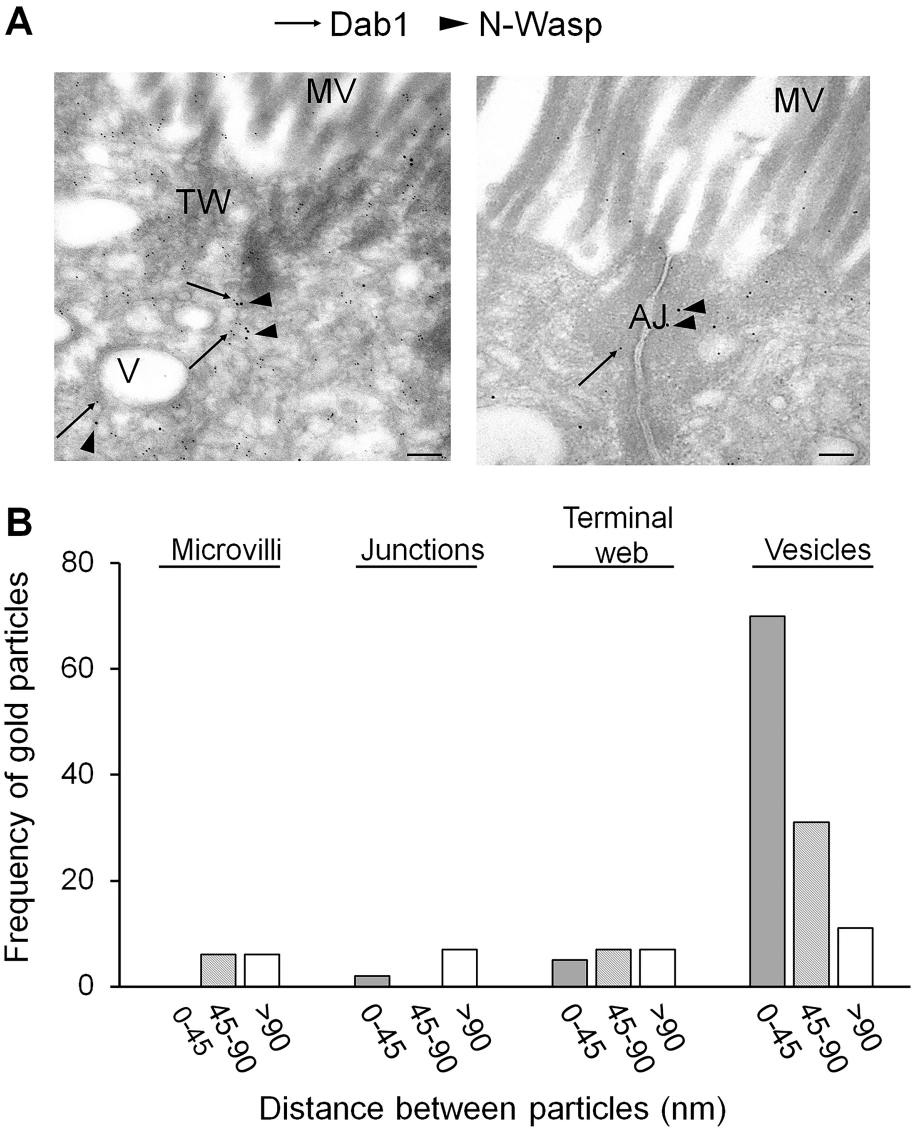
A
Dab1
N-Wasp
MV
TW
V
MV
AJ
B
Microvilli
Junctions
Terminal web
Vesicles
Frequency of gold particles
80
60
40
20
0
0-45
45-90
>90
Distance between particles (nm)

Figure 6

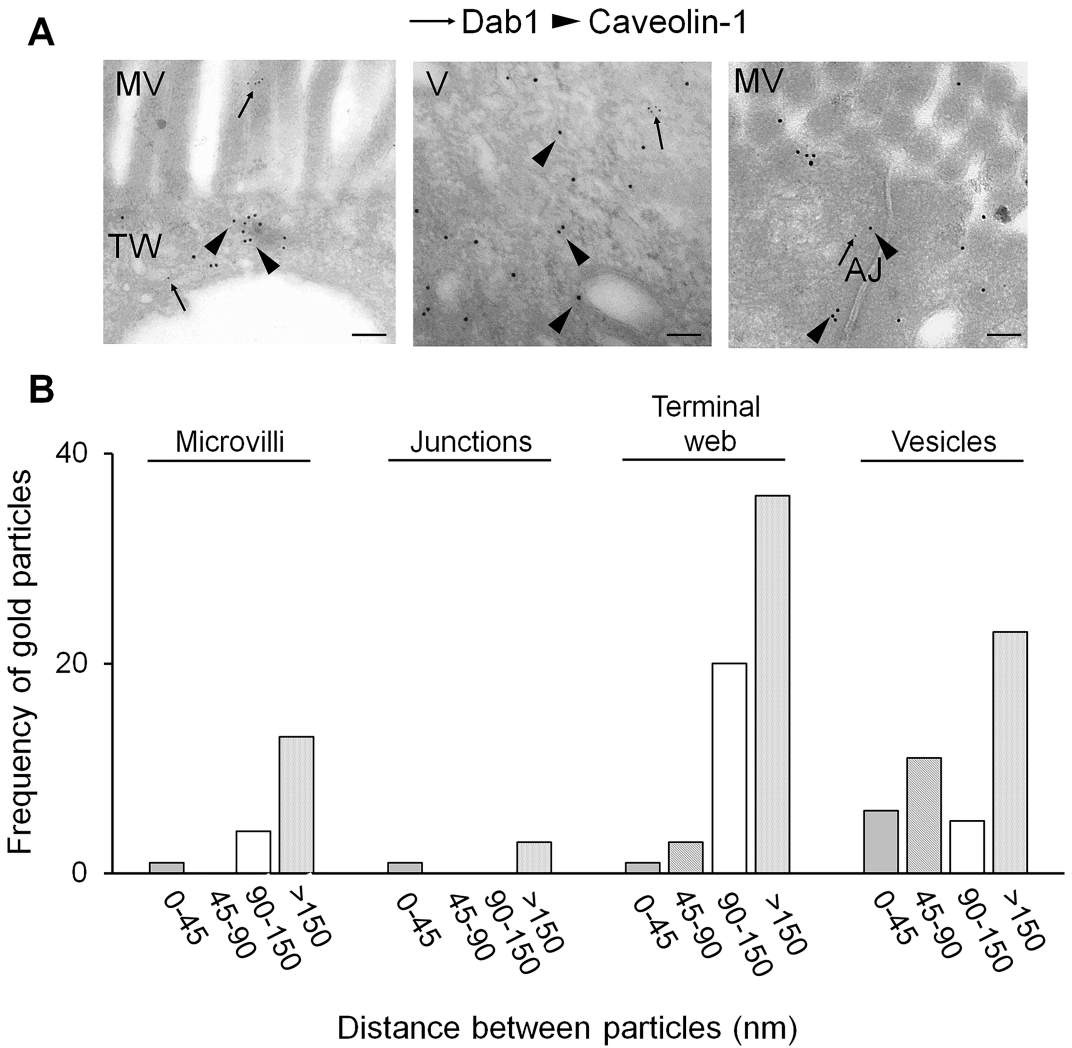
A
Dab1
Caveolin-1
MV
TW
V
MV
AJ
B
Microvilli
Junctions
Terminal web
Vesicles
Frequency of gold particles
40
20
0
0-45
45-90
90-150
>150
Distance between particles (nm)

Figure 7

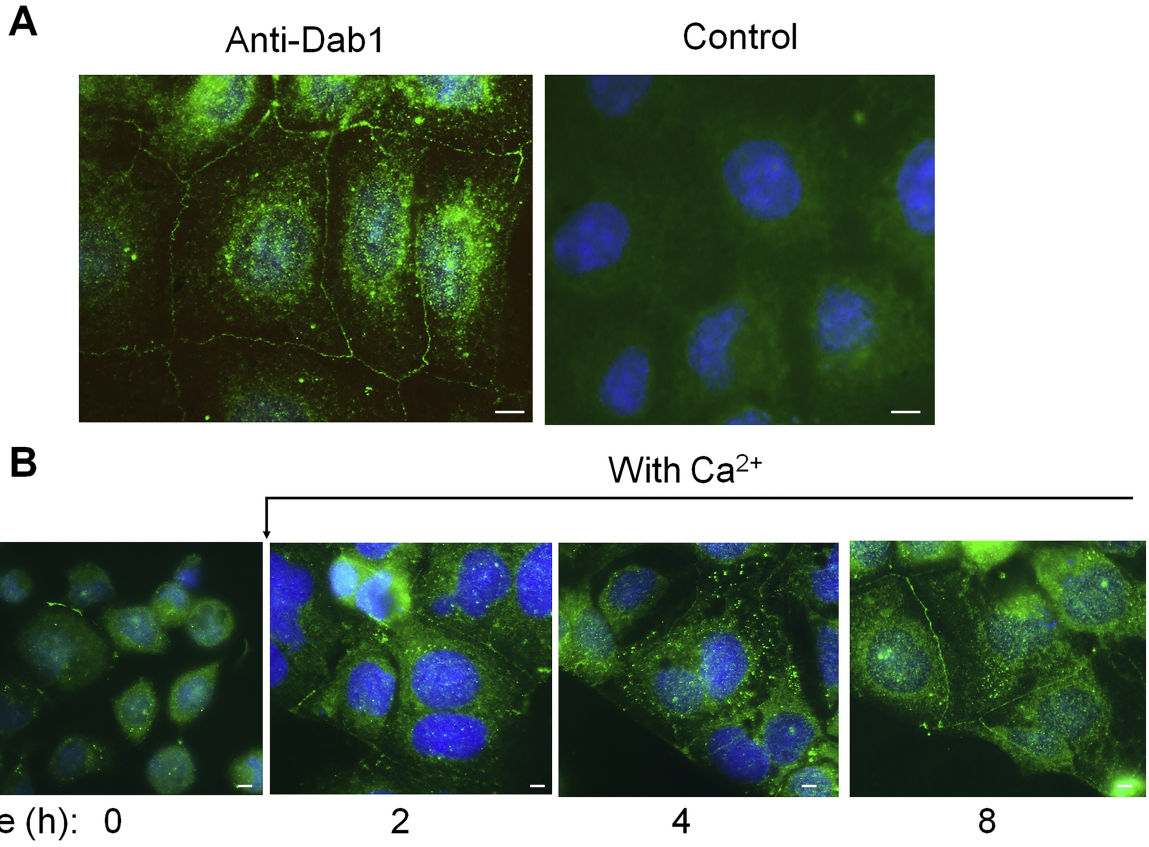

Figure 8